A New Mass Estimate of the Central Supermassive Black Hole in NGC 4051 with Reverberation Mapping

Kelly D. Denney[1]

ABSTRACT

There is increasingly strong evidence from observations of the local universe that every galaxy hosts a black hole at its center with a mass of hundreds of thousands to millions of times the mass of the sun. It is also becoming clear that these 'supermassive' black holes are connected to the evolution of galaxies. Therefore, understanding how galaxies form requires an understanding of the demographics of their central black holes. One of the few direct methods of measuring black hole masses in distant galaxies is to apply a technique known as reverberation mapping to objects that are actively accreting matter (active galactic nuclei or AGNs) and for which we have a generally unobscured view of the galactic nucleus (type 1 AGNs). Reverberation mapping takes advantage of an observed time delay between brightness fluctuations in light originating from a continuum source very near the black hole (the hot accretion disk) and broad emission lines (i.e., resolved in Doppler velocity) that are produced by rapidly moving gas in the vicinity of the nucleus, the broad-line emitting region (BLR). If the BLR gas is in virial equilibrium and under gravitational influence of the supermassive black hole, the velocity of the BLR gas, measured from the widths of broad emission lines, and the BLR radius are related through the mass of the black hole itself. Long observing campaigns monitor the continuum and emission-line brightness variations to measure the time delay, τ, which corresponds to the light travel time across the BLR. Measurements of τ then allow for an estimate of the size of the region, $R_{\rm BLR} = c\tau$, with which we can then estimate the black hole mass. We present the first results from a multi-month reverberation mapping campaign undertaken primarily at MDM Observatory but with supporting observations from telescopes around the world. We feature the results for NGC 4051 because it was previously

[1]Department of Astronomy, 140 W. 18th Ave, Columbus, OH 43221; denney@astronomy.ohio-state.edu; A token of thanks to my adviser Bradley M. Peterson and to B. Scott Gaudi for advice and comments on this manuscript.

found to be a significant outlier from the relationship between the BLR radius and the optical continuum luminosity, the $R_{\rm BLR}$–L relationship, found for other AGNs. We measure a relatively small BLR radius and thus black hole mass for NGC 4051 that would have been impossible for past studies to resolve because the variations were previously undersampled. Our new results indicate that this AGN is actually completely consistent with the $R_{\rm BLR}$–L relationship, thus resolving the previous discrepancy and strengthening the evidence for the homologous nature of AGNs — an exciting interpretation of the tightness of the $R_{\rm BLR}$–L relationship, given the diverse demographics of galaxies.

1. Introduction

Recent theoretical and observational studies have provided strong evidence suggesting a connection between supermassive black hole growth and galaxy evolution (e.g., Bennert et al. 2008; Somerville et al. 2008; Hopkins & Hernquist 2008; Shankar et al. 2009). To better understand this connection, we need more direct measurements of supermassive black hole (SMBH) masses across cosmological distances. One way to measure the masses of SMBHs in distant galaxies is to use the technique of reverberation mapping (Blandford & McKee 1982; Peterson 1993), which may be applied to galaxies which host type 1 Active Galactic Nuclei (AGNs). In these types of galaxies, material is 'actively' accreting onto the SMBH in the nucleus of the galaxy. Reverberation mapping (RM) relies on properties of this accreting matter to infer properties of the SMBH itself, including its mass, and has been used to measure the mass of the SMBH in more than three dozen type 1 AGNs to date.

RM takes advantage of the presence of a time delay, τ, between light being emitted from the material falling into the black hole from an accretion disk, called continuum emission, and light in the form of Doppler-broadened emission lines being emitted by specific species of atoms in a region called the broad line region (BLR), located anywhere from a few to hundreds of light days from the SMBH. This time delay corresponds to the light travel time across the BLR, and thus measurements of τ provide an estimate of the size of the region, $R_{\rm BLR} = c\tau$. Because the BLR gas is well within the sphere of influence of the black hole and studies have provided evidence for

virialized motions within this region (e.g., Peterson et al. 2004, and references therein), $R_{\rm BLR}$ can be related to the mass of the SMBH through the velocity dispersion of the BLR gas, which can be estimated from a measure of the width of the emission line. In this way, the mass of the black hole can be defined by

$$M_{\rm BH} = \frac{f c\tau (\Delta V)^2}{G}, \tag{1}$$

where τ is the measured emission-line time delay, so that, again, cτ represents the BLR radius, and ΔV is the BLR velocity dispersion. The dimensionless factor f depends on the structure, kinematics, and inclination of the BLR and is of order unity.

Although RM is invaluable for measuring SMBH masses in both nearby and distant galaxies, this method is observationally taxing, since it requires months to years of spectroscopic monitoring to collect enough data to measure the time delay. Therefore, it is currently impossible to measure SMBH masses directly for large statistical samples of galaxies. However, the direct mass measurements made so far have led to the discovery of scaling relationships that relate SMBH mass to other galaxy or AGN observables that can be used to investigate the connection between SMBH mass and galaxy evolution. Some relations show connections between properties of the SMBH (i.e., its mass) and global properties of the host galaxy. Examples include the correlation between SMBH mass and velocity of stars in the bulge of the host galaxy, i.e. the $M_{\rm BH}$–$\sigma_\star$ relation for AGNs (Gebhardt et al. 2000b; Ferrarese et al. 2001; Onken et al. 2004; Nelson et al. 2004) and quiescent galaxies (Ferrarese & Merritt 2000; Gebhardt et al. 2000a; Tremaine et al. 2002), and the correlation between SMBH mass and the luminosity coming from the bulge of the galaxy (Kormendy & Richstone 1995; Magorrian et al. 1998; Wandel 2002; Graham 2007; Bentz et al. 2009b).

Other relations connect various AGN properties. One such relation is the correlation between black hole mass and optical luminosity (Kaspi et al. 2000; Peterson et al. 2004), which relates directly to how fast and efficiently the black hole is accreting matter and, in turn, producing luminous radiation. There is also a correlation between BLR radius and AGN luminosity, i.e., the $R_{\rm BLR}$–L relation (Kaspi et al. 2000, 2005; Bentz et al. 2006, 2009a), which is a statement about

the similarity of the nuclear environment and ionization physics within all AGNs. Since the line emission observed from the BLR is a result of photoionization by the continuum luminosity, the physics would naively suggest that there should be a simple relation between the luminosity of the continuum and the distance from the source of this radiation to the particles that it ionizes. This relation is actually observed in measurements of the AGN luminosity and BLR radii from reverberation mapping and has therefore proven to be very powerful for making indirect SMBH mass estimations (e.g., Vestergaard 2002, 2004; Corbett et al. 2003; Kollmeier et al. 2006; Vestergaard et al. 2008; Shen et al. 2008a,b; Fine et al. 2008) as follows: A single spectrum provides (1) a measurement of the luminosity, which leads to a BLR radius estimate through the $R_{\rm BLR}$–L relation, and (2) a measurement of the emission-line width, which, combined with the radius, leads to a black hole mass estimate. In this way, indirect mass measurements can be made for statistically large samples of AGNs. These masses can then be related to other properties of the host galaxy, through either separate scaling relationships or direct measurements of these properties, to study the evolutionary connection between the SMBH and the host galaxy.

Although scaling relations have become widely used for statistical studies, it is important to understand that the indirect mass estimates determined by these relations are only as reliable as the direct mass measurements used to calibrate them. Therefore, establishing a secure calibration across a wide dynamic range in parameter space and better understanding any intrinsic scatter in these relations is essential. To accomplish this, we must continue to make new direct measurements as well as to check previous results that are, for one reason or another, suspect.

NGC 4051 is a case in point. Measurements of the BLR radius and optical luminosity (Peterson et al. 2000, 2004) place it above the $R_{\rm BLR}$–L relation, i.e., the BLR radius is too large for its luminosity (cf. Figure 2 of Kaspi et al. 2005). It also appears to be accreting mass at a lower rate than other AGNs of similar properties. (cf. Figure 16 of Peterson et al. 2004). These two anomalies together suggest that perhaps the BLR radius has been overestimated by Peterson et al. (2000, 2004); indeed an independent reverberation measurement of the BLR radius in NGC 4051 by Shemmer et al. (2003) is about half the value measured by Peterson et al. (2000). Furthermore, neither the Peterson et al. nor Shemmer et al. data sets are particularly well sampled on short time

scales, so neither set is suitable for detection of smaller time lags.

In this work, we present an analysis of new observations of NGC 4051, which represent the first results from a densely sampled reverberation mapping campaign that began in early 2007. The campaign spanned more than 4 months, during which time we consistently obtained multiple photometric observations per night and spectroscopic observations nearly every night from a combination of five different observatories around the globe. The immediate goal of this work is to make improvements on the Hβ reverberation lag measurement for NGC 4051, since it is on the low-luminosity end of $R_{\rm BLR}$–L scaling relationship and has a poorly determined reverberation lag and, consequently, poorly determined black hole mass. Improving this measurement will help constrain the calibration of the $R_{\rm BLR}$–L scaling relationship, which, in turn, will help calibrate the indirect mass estimates used in large statistical studies to better understand galaxy evolution.

2. Observations and Data Analysis

Spectra of the nuclear region of NGC 4051 were obtained from both the 1.3-meter telescope at MDM Observatory and the 2.6-meter Shajn telescope of the Crimean Astrophysical Observatory (CrAO). These spectral observations targeted the Hβ $\lambda4861$ and [O III] $\lambda\lambda4959, 5007$ emission line region of the optical spectrum. Figure 1 shows the mean and rms spectra of NGC 4051 based on the MDM observations. The rms spectrum demonstrates how variable the flux was over the course of the campaign at any given wavelength and gives an indication of what emission lines have the most variability and are thus best to use for tracing a reverberation signal. Because we are searching for these variability signals in the flux from the AGN, calibrating the flux measured from all observations is very important. We performed a relative flux calibration separately for each set of spectra using the the algorithm of van Groningen & Wanders (1992). Following this method, we measure the flux from a portion of the spectrum that can be taken to have constant flux across the entire duration of the campaign. We then scale the whole spectrum so that this isolated portion has the same flux in every spectrum. Here, fluxes were calibrated by scaling them to the [O III] $\lambda5007$ narrow emission-line flux measured in the mean spectrum. We are able to base our flux calibration on this emission line because it originates in a low-density region much farther from the SMBH,

where it is not subject to the same conditions which cause the short timescale variable reverberation signal. The standard deviation in the mean [O III] $\lambda5007$ line flux after calibration demonstrates that our relative spectral flux calibration is good to $\sim$1.5%. Finally, we applied an absolute flux calibration to the MDM spectra by scaling to the absolute flux of the [O III] $\lambda5007$ emission line determined by Peterson et al. (2000).

In addition to spectral observations, we obtained V-band photometry from the 2.0-m Multicolor Active Galactic NUclei Monitoring (MAGNUM) telescope at the Haleakala Observatories in Hawaii, the 70-cm telescope of the CrAO, and the 0.4-m telescope of the University of Nebraska. Relative flux calibration of the photometric observations was performed by comparisons to standard stars of known brightness in the same field of view as NGC 4051.

All of these observations were combined into two light curves, which plot the flux as a function of time. First, the continuum light curve was created by combining all photometric observations and the average continuum flux density measured from all spectroscopic observations over the wavelength range 5090–5130 Å (see Fig. 1). Due to systematic differences between the various data sets, such as instrumental setup and data analysis practices, all observations are not on the same flux scale. Therefore, an flux scale factor was calculated for each data set to scale it to the MDM data set, which has been placed on an absolute flux scale as described above. The scale factor was calculated and applied to each set based on the difference in least squares fits between the MDM observations and each secondary set of observations. Next, since we are only interested in light originating from near the black hole, we subtracted the contribution coming from starlight in the host galaxy that is contaminating our continuum flux measurements. We calculated this contribution following the methods of Bentz et al. (2009a) by utilizing an image from the High Resolution Channel on the Advanced Camera for Surveys on board the *Hubble Space Telescope*. Finally, we binned closely spaced observations with a weighted average, applying this binning to continuum flux measurements separated by $\leq$0.25 day.

Light curves of the Hβ flux were made by integrating the flux in the Hβ emission line, defined in the MDM and CrAO spectra between 4815–4920 Å (see shaded region in Fig. 1). Before this integrated flux was measured, however, we subtracted a linearly interpolated continuum defined

between the average flux density in each of the follow regions on either side of Hβ: 4770–4780 Å and 5090–5130 Å. The CrAO Hβ light curve was then scaled to the MDM light curve using comparisons between contemporaneous data points (here, we define contemporaneous to be within 0.5 day). Finally, similar to the continuum flux measurements, Hβ emission line flux measurements separated by $\leq$0.5 day were binned. The final continuum and Hβ emission-line light curves are shown in Figure 2; Table 1 displays statistical parameters describing these light curves. Column (1) gives the spectral feature represented by each light curve, and the number of data points in each light curve is shown in column (2). Columns (3) and (4) are mean and median sampling intervals, respectively, between data points, and the mean flux with standard deviation is given in column (5).

3. Time Series Analysis

We performed a cross correlation analysis of the continuum and Hβ light curves to determine the most likely mean light travel time lag between continuum and emission line variations. For this analysis we employed an interpolation scheme (Gaskell & Sparke 1986; Gaskell & Peterson 1987) designed for unevenly spaced observations. We interpolated our light curves to simulate even spacing. We then calculate the correlation coefficient, r, between pairs of points from each light curve. We start with no lag and correlate the flux from the continuum with the flux from the emission line measured on the same night. Then, we build up a distribution of r values, called a cross-correlation function (CCF), by cross correlating the interpolated light curves after imposing a range of both positive and negative time lags, τ, on the Hβ light curve, by simply shifting it in time compared to the continuum light curve. The resulting CCF from this analysis of the NGC 4051 light curves is shown in Figure 3. We characterize the time delay between the continuum and emission line variations with $\tau_{\rm cent}$, which is the centroid of the CCF based on all points with $r \geq 0.8 r_{\rm max}$ (demonstrated by the shaded area in Fig. 3). We calculate $\tau_{\rm cent}$ to be $1.75^{+0.50}_{-0.68}$ days.

4. Black Hole Mass

We estimate the BLR velocity dispersion by the line width of the Hβ emission line. We characterize this width by the line dispersion, the second moment of the line profile, σ_{line}. We measured σ_{line} from the rms spectra of NGC 4051 shown in Figure 1 to be 916 ± 64 km s^{-1}. We use the width in the rms spectrum over that in the mean spectrum since we are only interested in the velocity of the BLR gas with variable brightness that is responsible for the reverberation signal.

We calculate the black hole mass for NGC 4051, using the values of $\tau_{\rm cent}$ we measured for the time delay, τ, and the line dispersion, $\sigma_{\rm line}$, for the emission-line width, ΔV. We use $\tau_{\rm cent}$ and $\sigma_{\rm line}$, as opposed to the other line width and time delay measures because because Peterson et al. (2004) argue that this combination of parameters gives the most reliable SMBH mass determinations, based on virial arguments and fits between all possible combinations of line width and time delay measures. We also adopt the scale factor of Onken et al. (2004), f=5.5, since it was derived using the same time delay and line width characterization to calibrate the reverberation mapping mass scale, making it consistent with SMBH masses in nearby inactive galaxies, such as the Milky Way, measured with other methods. With this set of parameters, we then use equation (1) to estimate the black hole mass of NGC 4051 to be $M_{\rm BH} = (1.58^{+0.50}_{-0.65}) \times 10^6 M_\odot$. Here, observational uncertainties have been included, but intrinsic uncertainties from sources such as unknown BLR inclination cannot be accurately ascertained.

5. Conclusion and Future Work

Using the lag measurement of $\tau_{cent} = 1.75^{+0.50}_{-0.68}$ days presented here, NGC 4051 is no longer an outlier on the $R_{\rm BLR}$–L relationship. Figure 4 replicates the most recent version of this relationship by Bentz et al. (2009a) with both the previous and current lag values of NGC 4051 marked. Secure placement of low-luminosity objects such as NGC 4051 on the $R_{\rm BLR}$–L relationship is important for supporting the extrapolation of this relationship to the even lower-luminosity regime potentially populated by intermediate-mass SMBHs. Additional results from the present campaign (Denney et al., in preparation), as well as results from a recent monitoring campaign at the Lick Observatory (e.g., Bentz et al. 2008), aim to further populate this low-luminosity end of the $R_{\rm BLR}$–

L relationship, thus solidifying the relationship over a larger range in luminosity than previously well-sampled. A reliable calibration of this relationship is imperative for large studies of black hole masses and galaxy evolution, since it allows for the calculation of black hole masses from single-epoch spectra and provides luminosity and radius estimates that help constrain parameter space in the search for intermediate-mass SMBHs.

Results for NGC 4051 from the reverberation campaign we have described here help to explain and update its placement on the $R_{\rm BLR}$–L relation, but we need more information than simply the average BLR lag to corroborate its position on other relations and learn more about the BLR, in general. For this effort, it is imperative that we better understand the structure and kinematics of the BLR, particularly the role systematic uncertainties, such as those due to BLR geometry, play in estimating SMBH masses, since this geometry affects the value of the scale factor, f, that goes into the mass calculation. Another goal is to better understand the accretion physics in this region and limit the effect object to object differences have on the scatter around and calibration of the various AGN–host scaling relations. Since the current diffraction limitations of even the largest telescopes make resolving such a small region as the BLR in even the nearest AGNs unlikely, future work will aim to utilize the data we have presented above to fully reconstruct the reverberation signal through what is called a 2D velocity–delay map. The reverberation lag measurement we presented above represents the average lag across the BLR, but because the BLR is really an extended region, gas in different locations of the BLR should respond to variations in the ionizing continuum flux on slightly different time scales. Measuring and mapping these slight differences in the BLR response time across velocity space produces this velocity–delay map (see Horne et al. 2004) and is an aspect of the reverberation mapping technique that has not yet been fully realized (though see Horne et al. 1991; Kollatschny 2003; Ulrich & Horne 1996, for previous attempts). Reconstructing the velocity-dependent reverberation response from the BLR in the form of a velocity–delay map is our best hope to gain insight into the geometry and kinematics of the BLR.

REFERENCES

Bennert, N., Canalizo, G., Jungwiert, B., Stockton, A., Schweizer, F., Peng, C. Y., & Lacy, M. 2008, ApJ, 677, 846

Bentz, M. C., Peterson, B. M., Netzer, H., Pogge, R. W., & Vestergaard, M. 2009a, ApJ, in press (astro-ph/0812.2283)

Bentz, M. C., Peterson, B. M., Pogge, R. W., & Vestergaard, M. 2009b, ApJ, in press (astro-ph/0812.2284)

Bentz, M. C., Peterson, B. M., Pogge, R. W., Vestergaard, M., & Onken, C. A. 2006, ApJ, 644, 133

Bentz, M. C., et al. 2008, ApJ, 689, L21

Blandford, R. D., & McKee, C. F. 1982, ApJ, 255, 419

Corbett, E. A., et al. 2003, MNRAS, 343, 705

Ferrarese, L., & Merritt, D. 2000, ApJ, 539, L9

Ferrarese, L., Pogge, R. W., Peterson, B. M., Merritt, D., Wandel, A., & Joseph, C. L. 2001, ApJ, 555, L79

Fine, S., et al. 2008, MNRAS, 390, 1413

Gaskell, C. M., & Peterson, B. M. 1987, ApJS, 65, 1

Gaskell, C. M., & Sparke, L. S. 1986, ApJ, 305, 175

Gebhardt, K., et al. 2000a, ApJ, 539, L13

—. 2000b, ApJ, 543, L5

Graham, A. W. 2007, MNRAS, 379, 711

Hopkins, P. F., & Hernquist, L. 2008, ApJ, in press, astro-ph/0812.2915

Horne, K., Peterson, B. M., Collier, S. J., & Netzer, H. 2004, PASP, 116, 465

Horne, K., Welsh, W. F., & Peterson, B. M. 1991, ApJ, 367, L5

Kaspi, S., Maoz, D., Netzer, H., Peterson, B. M., Vestergaard, M., & Jannuzi, B. T. 2005, ApJ, 629, 61

Kaspi, S., Smith, P. S., Netzer, H., Maoz, D., Jannuzi, B. T., & Giveon, U. 2000, ApJ, 533, 631

Kollatschny, W. 2003, A&A, 407, 461

Kollmeier, J. A., et al. 2006, ApJ, 648, 128

Kormendy, J., & Richstone, D. 1995, ARA&A, 33, 581

Magorrian, J., et al. 1998, AJ, 115, 2285

Nelson, C. H., Green, R. F., Bower, G., Gebhardt, K., & Weistrop, D. 2004, ApJ, 615, 652

Onken, C. A., Ferrarese, L., Merritt, D., Peterson, B. M., Pogge, R. W., Vestergaard, M., & Wandel, A. 2004, ApJ, 615, 645

Peterson, B. M. 1993, PASP, 105, 247

Peterson, B. M., et al. 2000, ApJ, 542, 161

—. 2004, ApJ, 613, 682

Russell, D. G. 2003, astro-ph/0310284

Shankar, F., Weinberg, D. H., & Miralda-Escudé, J. 2009, ApJ, 690, 20

Shemmer, O., Uttley, P., Netzer, H., & McHardy, I. M. 2003, MNRAS, 343, 1341

Shen, J., Vanden Berk, D. E., Schneider, D. P., & Hall, P. B. 2008a, AJ, 135, 928

Shen, Y., Greene, J. E., Strauss, M. A., Richards, G. T., & Schneider, D. P. 2008b, ApJ, 680, 169

Somerville, R. S., Hopkins, P. F., Cox, T. J., Robertson, B. E., & Hernquist, L. 2008, MNRAS, 391, 481

Tremaine, S., et al. 2002, ApJ, 574, 740

Ulrich, M.-H., & Horne, K. 1996, MNRAS, 283, 748

van Groningen, E., & Wanders, I. 1992, PASP, 104, 700

Vestergaard, M. 2002, ApJ, 571, 733

—. 2004, ApJ, 601, 676

Vestergaard, M., Fan, X., Tremonti, C. A., Osmer, P. S., & Richards, G. T. 2008, ApJ, 674, L1

Wandel, A. 2002, ApJ, 565, 762

Table 1. Light Curve Statistics

Time Series (1)	N (2)	Sampling Interval(days) $\langle T \rangle$ (3)	$T_{\rm median}$ (4)	Mean Flux[a] (5)
5100 Å	186	0.71	0.57	4.5 ± 0.4
Hβ	100	1.17	1.00	4.3 ± 0.3

[a]Units of flux are (10^{-15} erg s^{-1} cm^{-2} Å^{-1}) and (10^{-13} erg s^{-1} cm^{-2}) for 5100 Å continuum and Hβ, respectively.

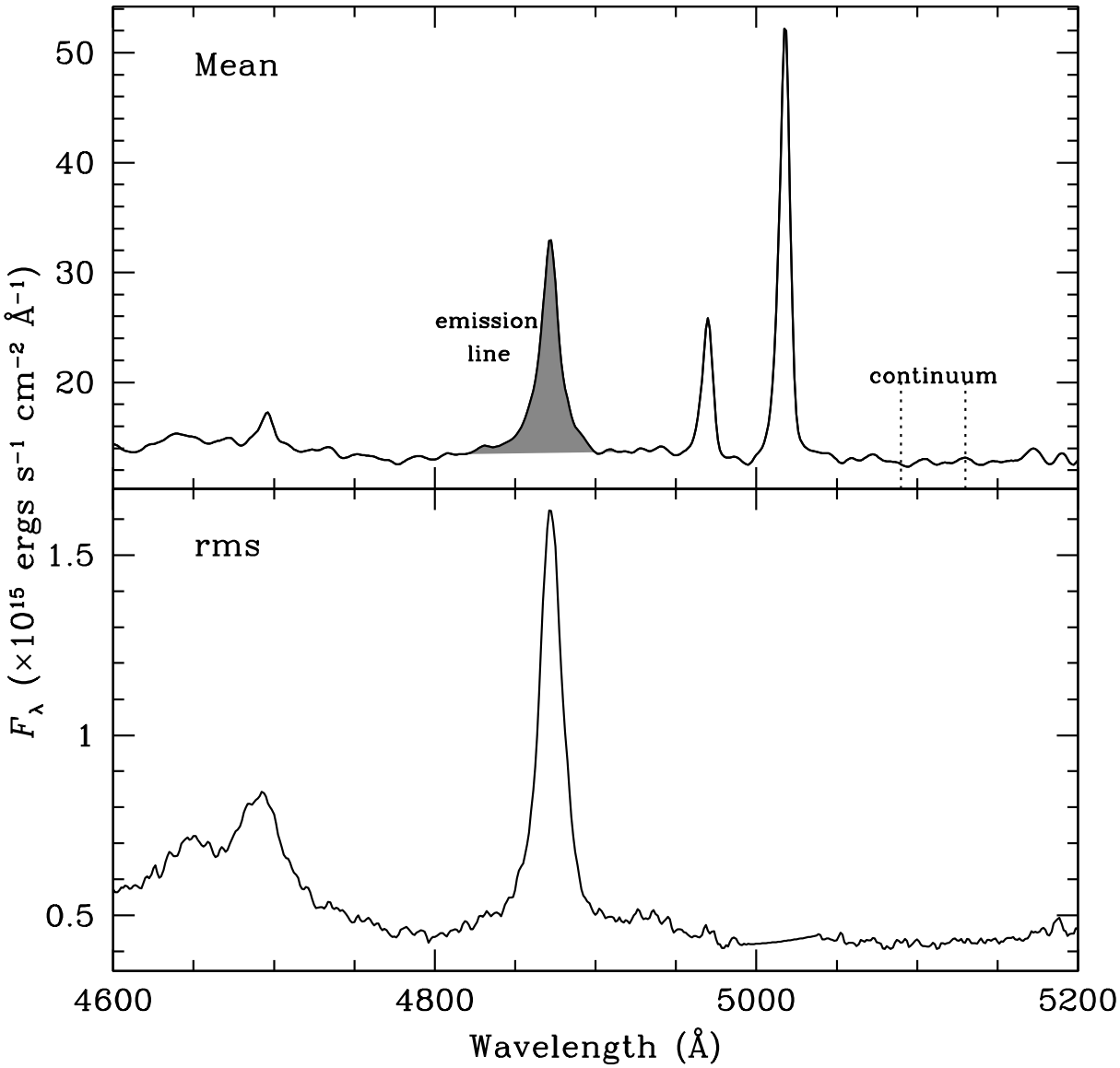

Fig. 1.— Mean and rms spectra of NGC 4051 from MDM observations. The rms spectrum was formed after removing the [O III] $\lambda 4959$ and [O III] $\lambda 5007$ narrow emission lines. The variability signature of Hβ is clearly visible in the rms spectrum, and the large increase in rms flux shortward of 4800 Å is due to variations in the broad He II $\lambda 4686$ emission line. The shaded region defines the Hβ emission line region from which we measured the integrated flux for the emission-line light curve, and the vertical dotted lines show the boundaries between which we measured the average flux density for the continuum light curve.

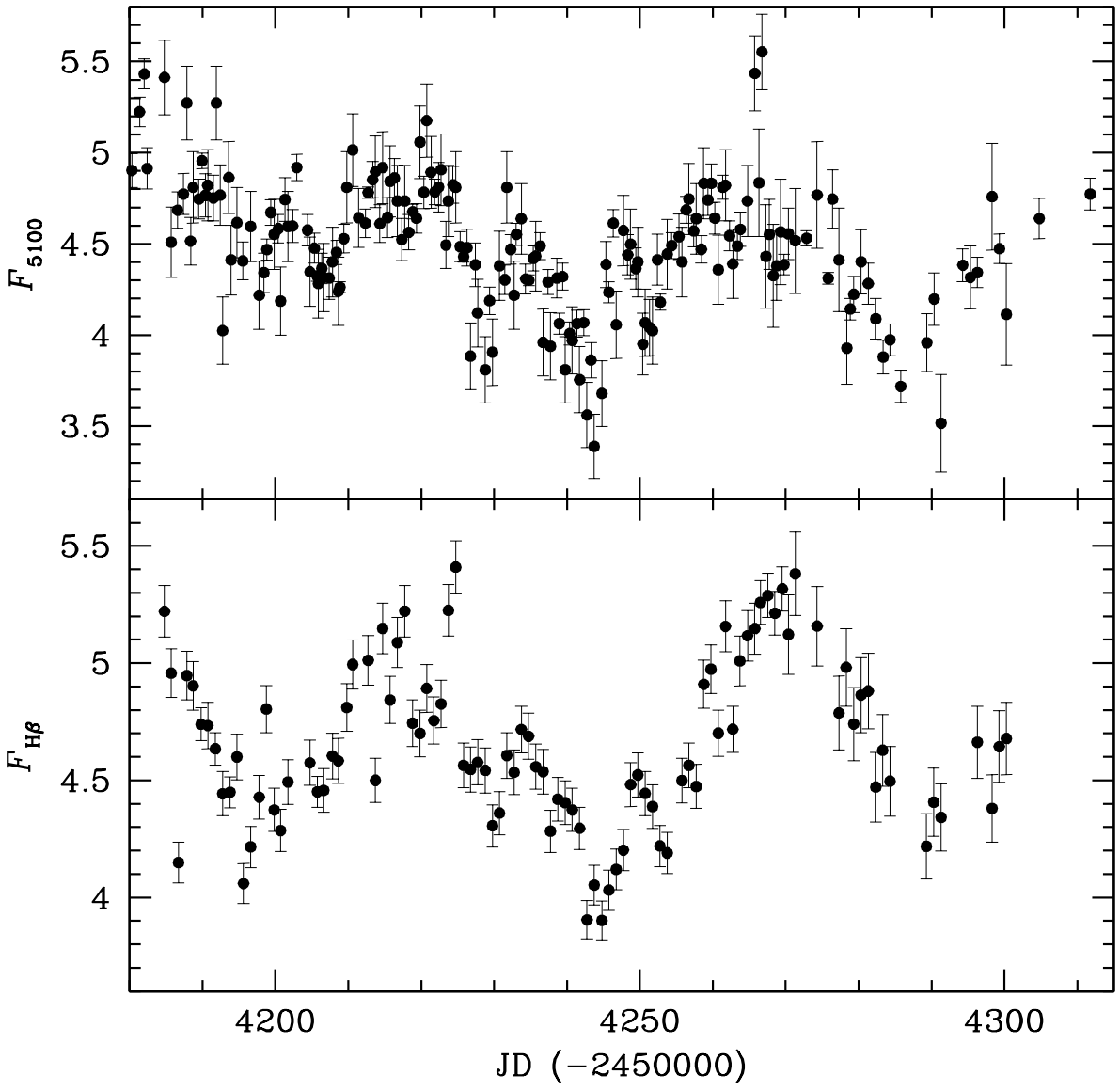

Fig. 2.— Light curves showing merged and time binned observations from all sources. The top panel shows the 5100 Å continuum flux in units of 10^{-15} erg s^{-1} cm^{-2} Å^{-1}, while the bottom is the Hβ λ4861 line flux in units of 10^{-13} erg s^{-1} cm^{-2}. Closely spaced observations were binned such that weighted averages were calculated for continuum observations separated by less than 0.25 day and Hβ observations separated by less than 0.5 day.

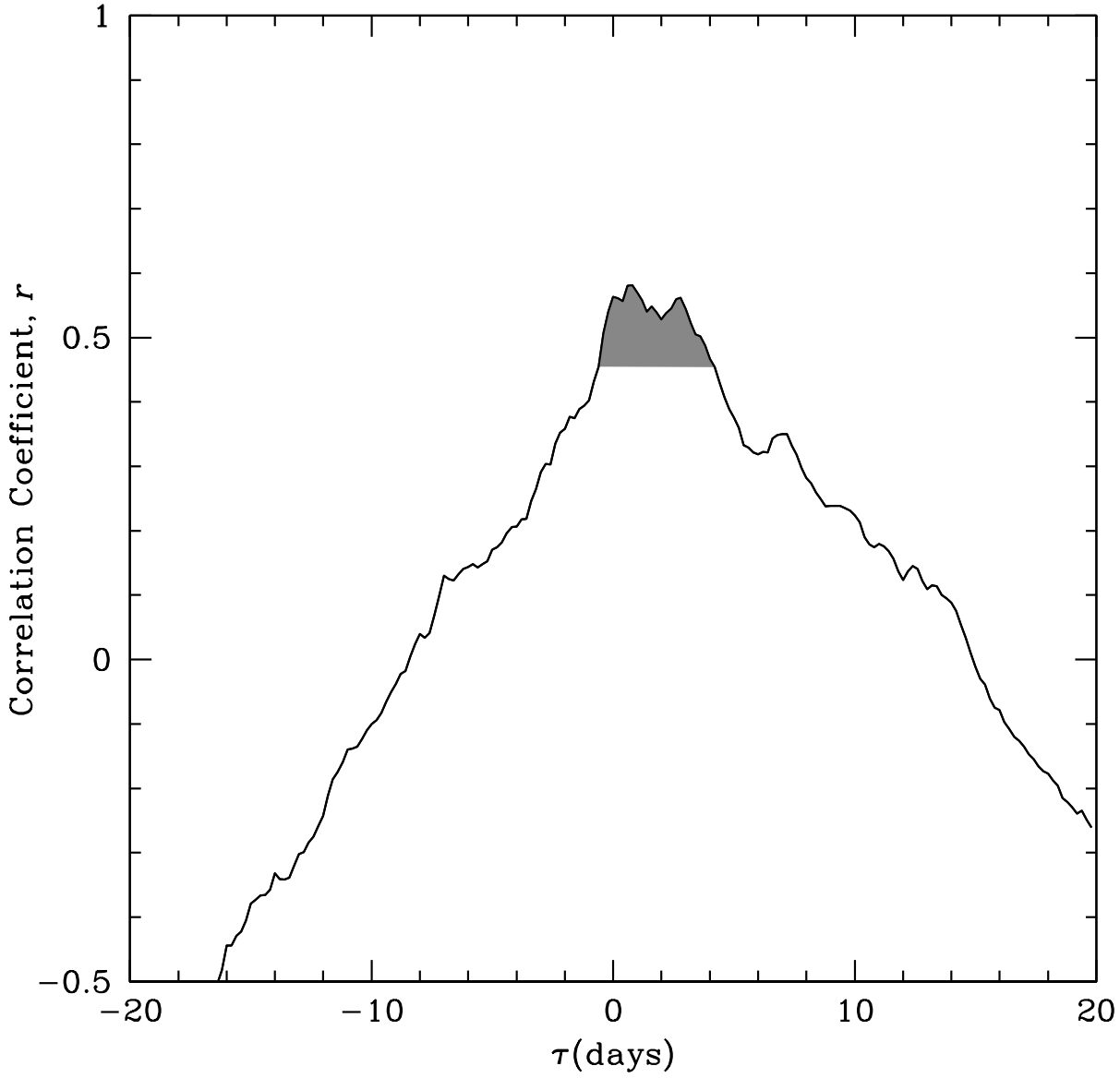

Fig. 3.— Cross correlation function from time series analysis of the continuum and Hβ light curves of NGC 4051 shown in Fig. 2. The shaded region represents the area used for the centroid calculation to determine $\tau_{\rm cent}$.

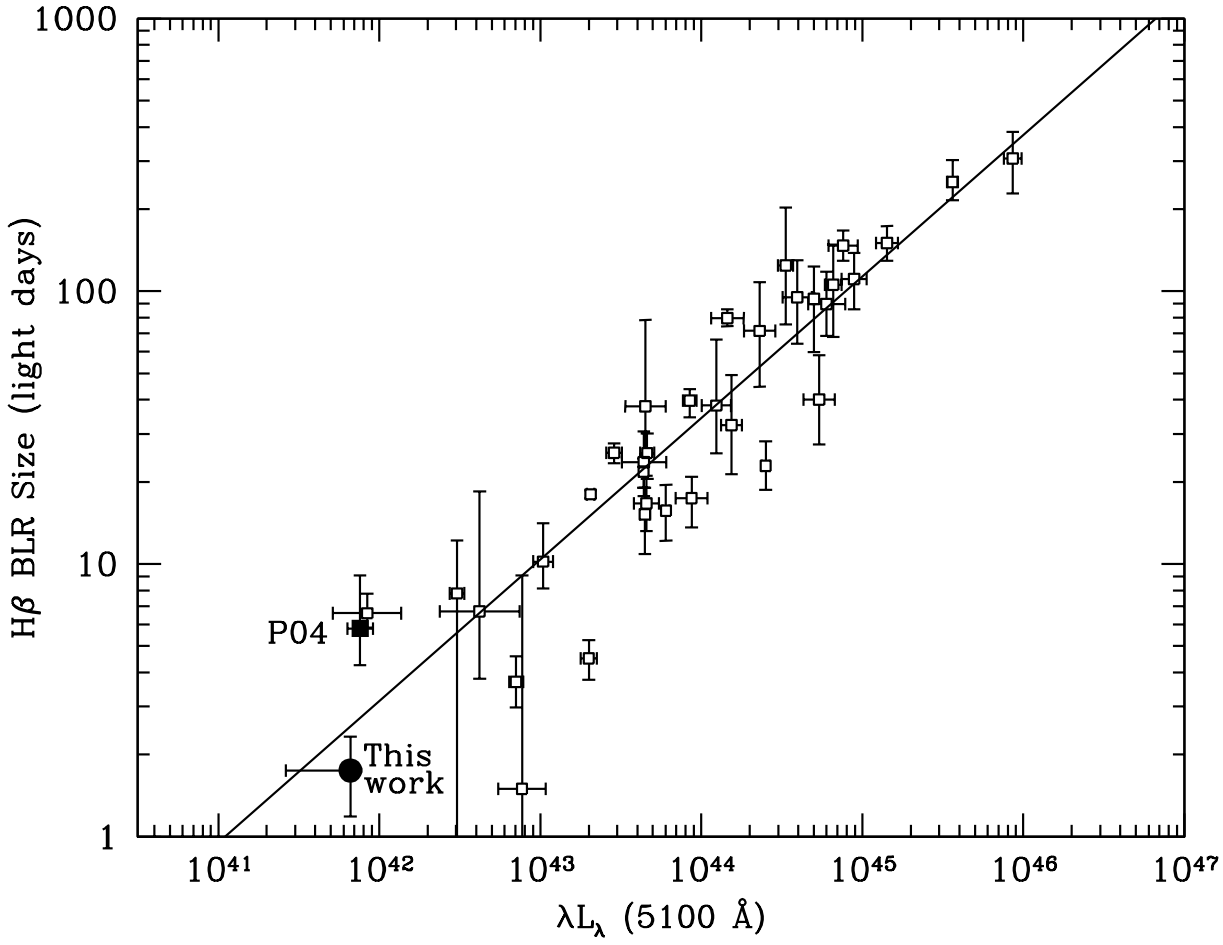

Fig. 4.— Most recently calibrated $R_{\rm BLR}$–L relation (Bentz et al. 2009a, solid line). The filled square shows the location of NGC 4051 based on results from Peterson et al. (2004) and used by Bentz et al. The filled circle shows the new lag measurement of 1.75 days presented in this work. The uncertainty in luminosity for our current result is a combination of the dispersion in luminosity during our campaign and the uncertainty due to the difference in the distance to NGC 4051 between that inferred from the redshift of this object and our adopted Tully-Fisher distance (Russell 2003). Open squares represent other objects from Bentz et al. (2009a).